NASA TECHNICAL MEMORANDUM

NASA TM X-2426

NASA TM X-2426

DESIGN AND TWO-DIMENSIONAL CASCADE TEST OF A JET-FLAP TURBINE STATOR BLADE WITH RATIO OF AXIAL CHORD TO SPACING OF 0.5

by Roy G. Stabe

Lewis Research Center
Cleveland, Ohio 44135

NATIONAL AERONAUTICS AND SPACE ADMINISTRATION • WASHINGTON, D. C. • DECEMBER 1971

1. Report No.	2 Government Accession No	3 Recipient's Catalog No
NASA TM X-2426		

4. Title and Subtitle	5 Report Date
DESIGN AND TWO-DIMENSIONAL CASCADE TEST OF A JET-FLAP TURBINE STATOR BLADE WITH RATIO OF AXIAL CHORD TO SPACING OF 0.5	November 1971
	6. Performing Organization Code
7. Author(s)	8. Performing Organization Report No
Roy G. Stabe	E-6479
	10. Work Unit No.
9. Performing Organization Name and Address	764-74
Lewis Research Center National Aeronautics and Space Administration Cleveland, Ohio 44135	11. Contract or Grant No
	13. Type of Report and Period Covered
12 Sponsoring Agency Name and Address	Technical Memorandum
National Aeronautics and Space Administration Washington, D.C. 20546	14 Sponsoring Agency Code

15 Supplementary Notes

16. Abstract

A jet-flap blade was designed for a velocity diagram typical of the first-stage stator of a jet engine turbine and was tested in a simple two-dimensional cascade of six blades. The principal measurements were blade surface static pressure and cross-channel surveys of exit total pressure, static pressure, and flow angle. The results of the experimental investigation include blade loading, exit angle, flow, and loss data for a range of exit critical velocity ratios and three jet flow conditions.

17 Key Words (Suggested by Author(s))	18 Distribution Statement
Jet engine turbine, Turbine blades, Jet flap blades, Low solidity, High loading	Unclassified - unlimited

19 Security Classif (of this report)	20 Security Classif (of this page)	21 No of Pages	22 Price*
Unclassified	Unclassified	21	$3.00

* For sale by the National Technical Information Service, Springfield, Virginia 22151

DESIGN AND TWO-DIMENSIONAL CASCADE TEST OF A JET-FLAP TURBINE STATOR BLADE WITH RATIO OF AXIAL CHORD TO SPACING OF 0.5

by Roy G. Stabe

Lewis Research Center

SUMMARY

The design of a very low solidity turbine jet-flap stator blade is described, and the results of an experimental investigation of this blade are presented. The blade was designed for a velocity diagram typical of the first stage of a jet engine turbine. The performance of the blade was investigated experimentally in a simple two-dimensional cascade of six blades. Two of these blades were instrumented with static taps to determine blade surface pressures. Surveys of blade exit total pressure, static pressure, and flow angle were made to define blade exit flow conditions. The blades were tested over a range of exit critical velocity ratios and at three jet flow conditions: no jet flow and jet to inlet total pressure ratios of 1.0 and 1.5.

With zero jet flow, the flow remained attached to the suction surface of the blades up to ideal exit critical velocity ratios $(V/V_{cr})_{id,3}$ of about 0.7. At higher exit velocity ratios the suction surface flow (without the jet) was separated. A jet to inlet total pressure ratio p_j'/p_1' of 1.0 effected reattachment and maintained attached flow up to the highest ideal exit critical velocity ratio investigated, which was 0.9.

The jet had a large influence on the turning of the flow and on weight flow and blade loading. Increased jet flow increased the turning and decreased both the weight flow and the blade loading. However, high blade loadings were obtained at all jet flow conditions. The thermodynamic loss at design exit critical velocity ratio and a jet pressure ratio of 1.0 was 4.2 percent of the ideal exit kinetic energy. The corresponding loss of the conventional solidity stator blade which served as a model for the jet flap blade was 2.5 percent at the mean section.

INTRODUCTION

The NASA Lewis Research Center is investigating advanced concepts to increase turbine blade loading. The use of highly loaded blading effects a reduction in turbine size

and weight through the use of fewer stages, a smaller diameter, or fewer blades. As the number of blades (the solidity) decreases, the force or loading on each blade must, of course, increase. The higher loading is evidenced by higher velocity on the suction surface of the blades and also by larger deceleration or diffusion. This larger diffusion is associated with higher loss and eventual flow separation. The design of highly loaded blading thus depends on the minimization of diffusion and its effects.

Diffusion is minimized by using high effective loading. This approach was used in the design of the low-solidity stator blade of reference 1. Boundary layer growth and separation are minimized by using boundary layer control devices. References 2 to 5 are representative of studies made on two such devices, namely, tandem and jet-flap blades.

This report is concerned with the performance of a turbine stator blade designed for very low solidity by using both a jet-flap and high loading effectiveness. On the jet-flap blade, a jet of air is injected into the main stream from the pressure surface near the trailing edge. The jet forms an aerodynamic flap which deflects the flow, thereby changing the circulation around the blade and increasing the blade loading. The jet also entrains the boundary layer and reduces its thickness. A thinner boundary layer inhibits separation and allows a higher diffusion. The jet-flap blade is also attractive because in a high temperature application the cooling air may also be used for the jet. In addition, because the jet deflects the flow, the jet-flap could be used for a variable area device.

As in the case of the low solidity plain stator blade of reference 1, the design of the jet-flap blade was based on the stator blade described by Whitney (ref. 6). These blades which were designed for a velocity diagram typical of the first-stage stator of a jet engine turbine, yielded an efficiency of 0.965. The solidity, based on axial chord, was 1.0 at the mean radius. This solidity is less than the optimum value obtained from such standard references as Zweifel (ref. 7) or Miser, Stewart, and Whitney (ref. 8). The solidity of the jet-flap blade was reduced to 0.5, which is one-half that of Whitney's blade. For the same velocity diagram, this is equivalent to doubling the blade loading. The purpose of the program, then, was to design blades that achieve this very high loading without sacrificing the high efficiency of the reference blade.

The performance of the jet-flap blades was investigated experimentally in a simple two-dimensional cascade of six blades. The principal measurements were blade surface static pressure and cross-channel surveys of exit total pressure, static pressure, and flow angle. These data were taken at several ideal exit critical velocity ratios between approximately 0.6 and 0.9. At each critical velocity ratio data were taken for zero jet flow and for jet-to-inlet total pressure ratios of 1.0 and 1.5. The results of the experimental investigation include exit survey results, blade loading in terms of blade surface pressures, and overall performance in terms of exit flow angles, mass flow, loss, and blade loading coefficients.

SYMBOLS

a	distance along axial chord from blade leading edge, cm
C_a	blade axial chord, cm
D_s	blade suction surface diffusion factor, $(p_1' - p_{s,min})/p_1' - p_3)$
$\bar{e}_{3P}$	primary kinetic energy loss coefficient, $1 - \left[W_3 V_3^2 / W_P (V_{id,3})_P^2\right]$
$\bar{e}_{3T}$	thermodynamic kinetic energy loss coefficient, $1 - \left\{W_3 V_3^2 / \left[W_P (V_{id,3})_P^2 + W_J (V_{id,3})_J^2\right]\right\}$
m	mass flow rate per unit area, kg/sec-cm^2
p	absolute pressure, N/cm^2
s	blade spacing, cm
t	tangential distance from blade trailing edge, cm
V	velocity, cm/sec
W	flow rate per cm of blade span, kg/sec-cm
α	flow angle, deg from axial
ψ_z	Zweifel loading coefficient for compressible flow

Subscripts:

cr	flow conditions at Mach 1
id	ideal or isentropic process
J	jet
min	minimum value
P	primary
s	blade suction surface
1	station at blade inlet
2	station at blade exit survey plane
3	station at blade exit where flow conditions are assumed uniform

Superscript:

'	total state condition

BLADE DESIGN

The same procedure and specification were used to design the jet-flap blades as to design the low solidity plain stator blade of reference 1. The velocity diagrams were typical of the mean section of a first-stage stator for a jet engine turbine and the solidity based on axial chord was also 0.5.

The blade profile was designed to maintain high velocities along the length of the suction surface and low velocities along the length of the pressure surface. This velocity distribution minimizes diffusion. A computer program developed by Katsanis (ref. 9) was used to determine the blade surface velocities. The program solves the stream function equation by finite difference methods. The output includes surface velocities and blade-to-blade flow field velocities and angles.

The results obtained from this program are in good agreement with experimental results (ref. 1). The program input requires the blade geometry, weight flow, and the inlet and exit free stream flow angles.

When using this program for a jet-flap blade, it is necessary to know the deflection of the flow due to the jet to establish the blade angles at the trailing edge. At the time the jet-flap blades were designed, some of the information available on the jet-flap blade indicated that quite large deflections were possible. Accordingly, the blades were designed for a net deflection of the flow due to both jet and trailing edge blockage of 15.5°.

The jet slot was alined so that the jet would issue from the pressure surface normal to the downstream flow direction. The slot, which is 1 millimeter wide, was sized to provide a ratio of jet to primary free stream momentum of approximately 0.04 with a critical jet velocity.

During preliminary testing it was found that while the jet was effective in suppressing separation it was not nearly so effective in deflecting the flow as had been supposed in the design. The exit flow angles were much less than the design value. With enough jet flow to suppress separation, the exit flow angle was approximately equal to the mean blade angle.

The computer program of reference 9 was then used to determine the blade surface velocity distribution for larger stagger angles. It was found that the blade profile had an acceptable surface velocity distribution with a stagger angle 15° larger than the original design. New cascade end walls were made incorporating this larger stagger angle. The blade spacing was also changed to maintain the axial solidity at a value of 0.5. The resulting blade geometry and the velocity diagrams are shown in figure 1. The blade coordinates are given in table I.

The blades were fabricated of aluminum. The internal cavity was machined first in two parts roughly corresponding to the pressure and suction surface halves of the blade.

TABLE I. - STATOR BLADE COORDINATES

Upper surface coordinates, cm		Lower surface coordinates, cm	
X	Y_U	X	Y_L
0	0.635	0	0.635
.127	1.016	-----	------
.254	1.163	-----	------
.381	1.257	-----	------
.508	1.321	-----	------
.635	1.372	.635	0
.762	1.410	-----	------
1.016	1.455	1.016	.033
1.270	1.481	-----	------
1.524	1.491	1.524	.081
1.778	1.486	-----	------
2 032	1.468	2.032	.114
2.286	1.435	-----	------
2.540	1.392	2.540	.140
2 794	1.338	-----	------
3.048	1.275	3.048	.152
3.302	1.201	-----	------
3.556	1.118	3.556	.147
3.810	1.034	-----	------
4.064	.940	4.064	.124
4.318	.843	-----	------
4.572	.737	4.572	.084
4.826	.630	-----	------
5.080	.513	5.080	.0178
5.334	.274	5.220	0
5.378	.159	5.378	.159

These two blocks were electron-beam welded together forming the complete internal cavity. The external profile was then machined. Several webs 0.08 centimeter thick by 1.5 centimeter long and spaced 1.9 centimeters apart along the blade span were electron-beam welded to the suction and pressure surfaces. These webs strengthen the trailing edge and help aline the jet flow. The jet slot was cut along the active span of the blades at an angle normal to the downstream flow angle. This angle was not changed when the stagger angle was increased, so the blades were tested with the jet alined as shown in figure 1.

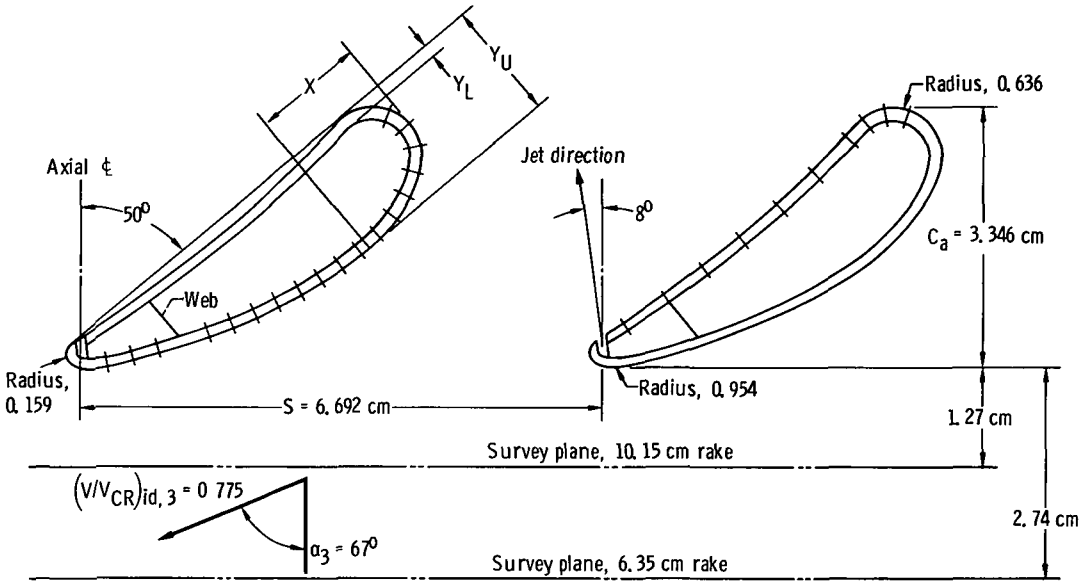

Figure 1. - Jet-flap stator blade geometry. (Location of blade surface taps is indicated by hash marks on blades.)

APPARATUS AND PROCEDURE

Cascade

The jet-flap blades were tested in a simple two-dimensional cascade of six blades. The cascade tunnel was essentially the same one used for the plain blade tests of reference 1. This cascade tunnel is shown installed in the test cell in figure 2.

The inlet guide walls were set to the approximate location of the inlet stagnation stream lines of the end blades. The exit guide walls were about 10 centimeters away from the end blades. (In this position it is assumed that the guide walls do not contribute substantially to the turning of the flow.) The spacing of the end walls or the blade length was 10.15 centimeters. Boundary layer suction was not used.

Air for the jet flaps was supplied to both ends of the blades from manifolds on the blade end walls. This was done to ensure an adequate supply of air for uniform jet flow over the blade span. An ASME flat plate orifice was used to measure the jet air flow.

In operation, room air was drawn through the cascade tunnel, blading, and exhaust control valve into the laboratory altitude exhaust system. The pressure ratio across the blades was maintained by regulation of the exhaust control valve. The blades were tested over a range of inlet total to exit static pressure ratios corresponding to exit ideal critical velocity ratios of approximately 0.6 to 0.9. Three jet flow conditions were set at each velocity ratio. These were the zero jet flow and jet-to-inlet total pressure ratios

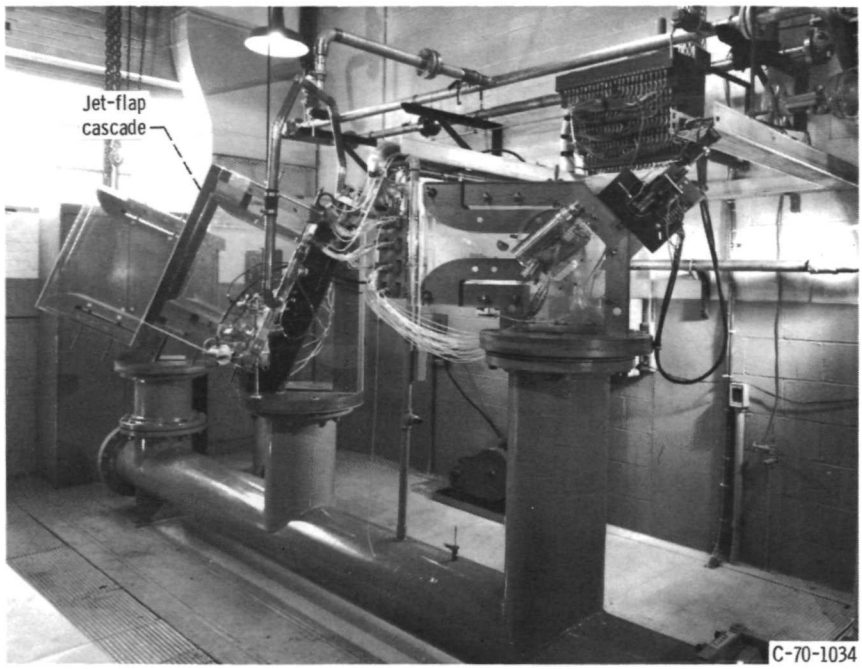

Figure 2. - Cascade tunnel installation.

p_j'/p_1' of 1.0 and 1.5. The jet total pressure was taken to be equal to the air supply manifold pressure. This pressure was set using a flow control valve in the jet air supply line.

Instrumentation

The two blades that formed the center channel of the cascade were instrumented at midspan with static pressure taps. The static tap diameter was 0.05 centimeter. The location of these taps is shown in figure 1. The cascade also had wall static taps in the inlet and exit sections. These taps were used to determine the uniformity of the flow and set exit static pressure. The blade surface and wall static pressures were measured with mercury filled manometers. The pressure data were recorded by photographing the manometer board.

The total pressure, static pressure, and flow angle at the exit of the center blade channel were surveyed simultaneously with a rake like the one shown in figure 3. The total pressure was measured with a simple square-ended probe made from 0.5-millimeter outside-diameter tubing with a wall thickness of 0.062 millimeter. The static pressure was measured with a wedge probe that had an included angle of 15°. The angle probe was the two-tube type made from tubing the same size as that of the total pressure

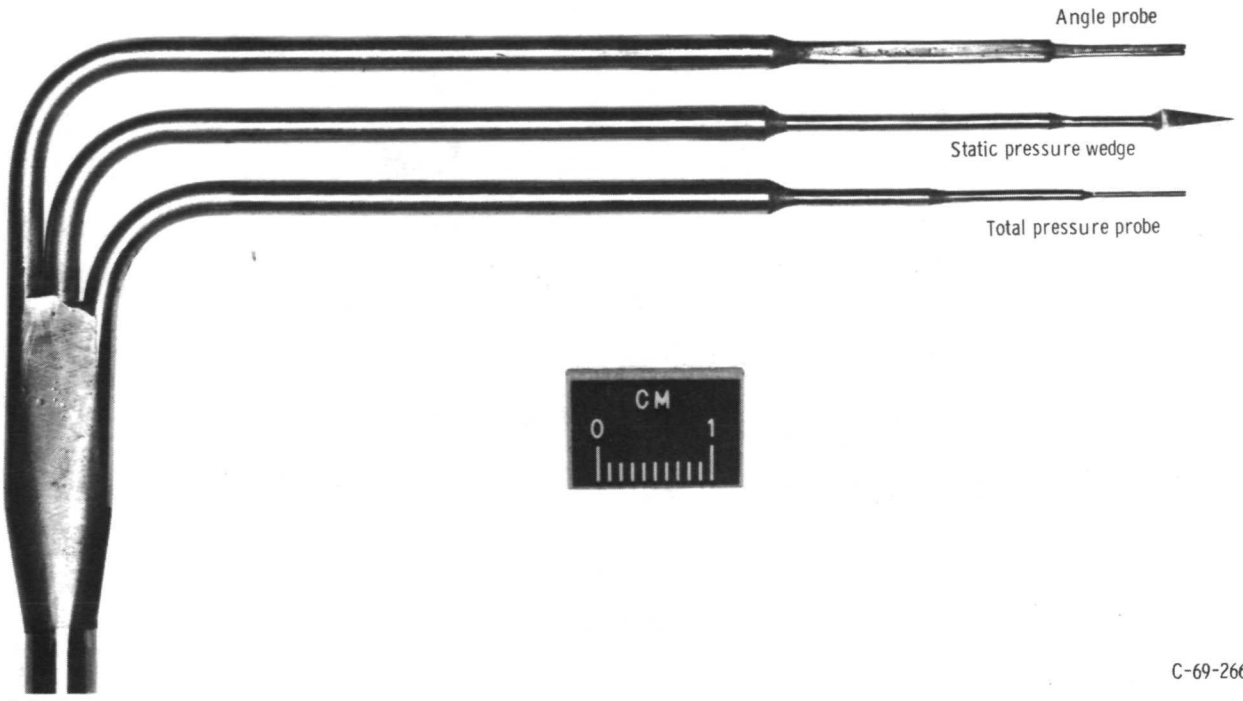

Figure 3. - Combination exit survey probe.

probe. The ends of the tubes are cut at 45^{o} so that the beveled ends of the tubes face each other and form an included angle of 90^{o}. The probe measures a differential pressure that is proportional to the flow angle. Strain-gage transducers were used to measure these pressures.

Two of these rakes were used; one was 10.15 centimeters long and the other was 6.35 centimeters long. The longer rake was used primarily to get good definition of the variations in the flow field near the trailing edge. Most of the data presented in the overall performance section is based on data taken with the shorter rake. In general, however, there was good agreement in the results calculated from data taken with either rake. The exception was in loss. Losses calculated from data taken with the shorter rake were slightly higher than with the long rake.

The rake was fixed at the design exit flow angle which placed the sensing elements at the appropriate survey plane shown in figure 1. The probe traversed 12.7 centimeters which was more than enough to cover the central channel and the two boundary wakes. The traverse speed was about 2.54 centimeters per minute. An actuator-driven potentiometer was used to provide a signal proportional to the rake position.

The output signals of the three pressure transducers were recorded as functions of rake position on x,y-recorders. The output signals of the three pressure transducers

and of the rake position potentiometer were recorded on magnetic tape. The recording rate was 20 words per second.

Data Reduction

Blade surface static pressures were taken from the photographs of the manometer board. These data were used to calculate the blade loading parameters. A computer was used to reduce the blade exit survey data recorded on magnetic tape. The flow angle, velocity, and flow per unit area were calculated from these data as functions of rake position. The weight flow, axial and tangential component of momentum, and static pressure were computed using a Simpson's rule integration over a distance equal to one blade space. The continuity and conservation of momentum and energy relations were then used to calculate the flow angle, velocity, and pressure at a hypothetical location where flow conditions were assumed uniform. This hypothetical location is designated station 3. For these calculations, the tangential component of momentum was assumed constant between the survey plane and station 3.

RESULTS AND DISCUSSION

The results of the investigation of the jet-flap blade performance in the two-dimensional cascade are presented in the Blade Exit Surveys, Blade Loading, and Overall Performance sections.

Blade Exit Surveys

The blade to blade variation of exit total and static pressure, flow angle, and mass flow for three jet flow rates are shown in figures 4(a), (b), and (c), respectively. These data were computed from measurements made with the long rake, that is, 1.27 centimeters axially downstream of the trailing edge. The data are for a nominal ideal exit critical velocity ratio of 0.7. This was the highest exit velocity for which there was no separation at zero jet flow.

The blade wakes are shown in the total pressure profiles of figure 4(a). Without jet flow the wake is sharply defined. With jet pressure ratios of 1.0 and 1.5 the wake becomes progressively broader and shallower. The jet does displace the wake tangentially. Most of the displacement of the wake is on the pressure surface side of the blade though there is some displacement toward the suction surface.

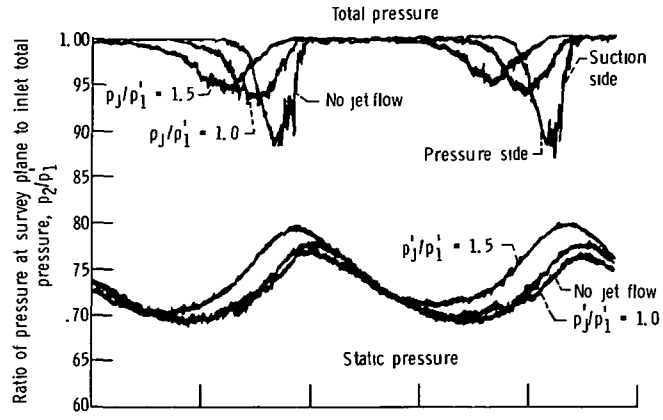

(a) Exit total and static pressures

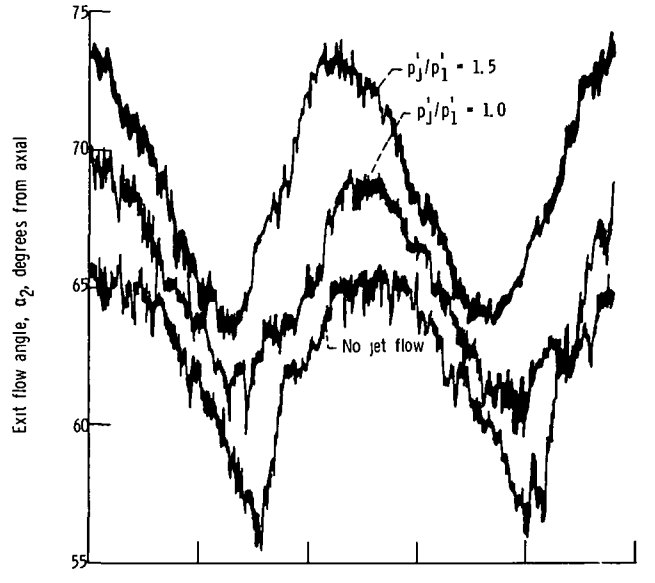

(b) Exit flow angle.

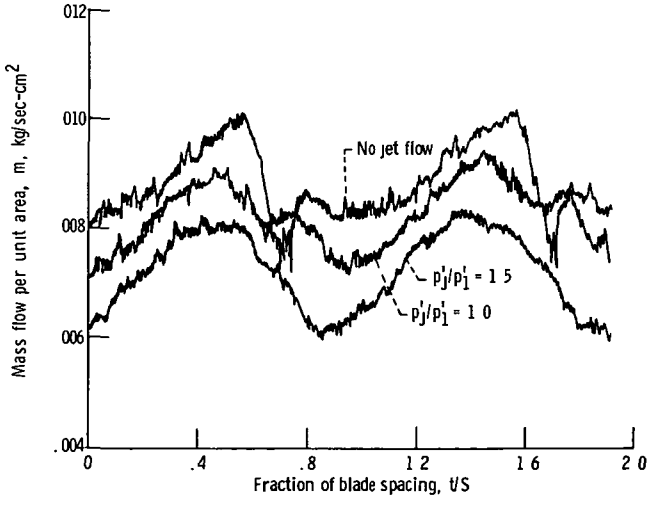

(c) Mass flow.

Figure 4. - Blade to blade variation of exit flow field. Nominal exit ideal critical velocity ratio, $(V/V_{CR})_{id,3}$, 0.7.

The static pressure variation is quite marked and amounts to about 10 percent of inlet total pressure. There is practically no tangential displacement of the static pressure profile between zero jet flow and a jet pressure ratio of 1.0. Some displacement toward the blade suction surface did occur when the jet pressure ratio was increased to 1.5.

The blade to blade variation in exit flow angle shown in figure 4(b) is also quite large, amounting to about 9° for all three jet flows. The effect of the jet on flow angle is not concentrated near the trailing edge of the blades. The angle of the entire flow field increases with jet flow yet there is comparatively little tangential displacement of either the static pressure or the angle profiles.

The blade to blade variations of static pressure and flow angle decreased considerably at greater distances downstream. Surveys made with the short rake, 2.74 centimeters axially downstream of the trailing edge, indicated that the static pressure variation was 2.5 percent of inlet total pressure and the angle variation was 3°.

The blade to blade variation in mass flow shown in figure 4(c) is quite similar to that of the flow angle as would be expected. The highest flow occurred at zero jet flow where the flow angle was closer to axial. The mass flow decreased throughout the entire flow field as jet flow was increased. The influence of the relatively well defined wake at zero jet flow is evident in the mass flow trace. The influence of the wake as evidenced by the traces decreases with increasing jet flow and vanishes a jet pressure ratio of 1.5.

The total pressure profiles for a nominal ideal exit critical velocity ratio of 0.8 are shown in figure 5. At this velocity with no jet flow the flow on the suction surfaces of the

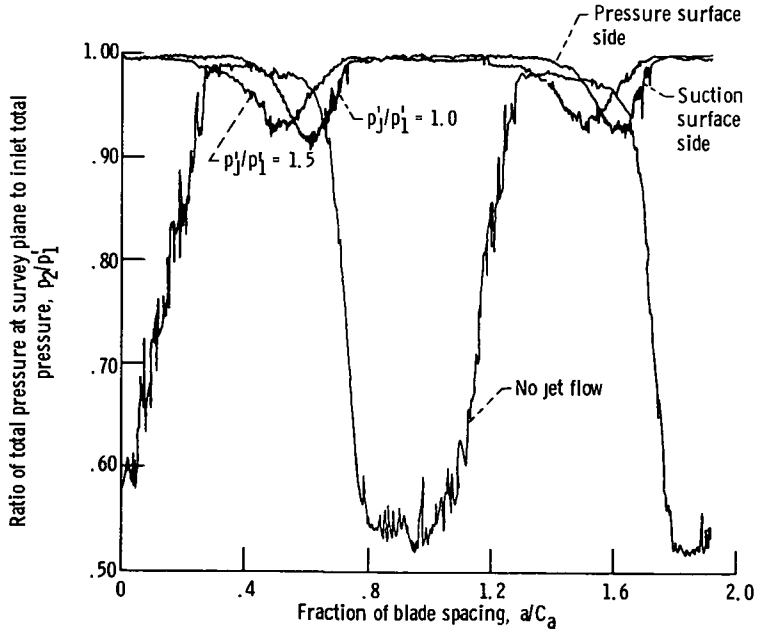

Figure 5. - Blade to blade variation of exit total pressure. Nominal exit ideal critical velocity ratio, $(V/V_{CR})_{id,3}$, 0.8.

blades was separated. And this is evident in figure 5. At a jet pressure ratio of 1.0 the flow is attached. The difference in the size of the two wakes and the amount of displacement towards the suction surface of the blade is dramatic. An increase in jet pressure ratio to 1.5 displaced the wake primarily on the pressure surface side of the blade as was the case at lower velocities.

During testing it was found that a jet pressure ratio of very nearly 1.0 was required to attach the flow at velocity ratios greater than about 0.7. And the transition from separated to attached flow was always abrupt.

Blade Loading

The blade loading distribution computed from blade surface static pressure measurements for three ideal exit critical velocity ratios and the three jet flow conditions investigated are shown in figure 6. It is convenient to express blade loading in terms of a blade surface pressure coefficient as in figure 6 because the area enclosed by the curves is equal to the Zweifel loading coefficient ψ_z. In addition, the maximum value of the pressure coefficient is equal to the suction surface diffusion factor D_s. The Zweifel coefficient is defined as the ratio of the tangential component of the blade pressure force to an ideal force based on the difference between the inlet total and exit static pressure acting on the axial chord.

The effect of the jet was to increase the loading on the pressure surface and decrease both the loading and diffusion on the suction surface. The net result was a decrease in blade loading with jet flow over the range of exit velocity ratios investigated.

For a given jet flow, the pressure coefficient profiles for the pressure surface are virtually identical for all three exit velocity ratios shown in figure 6. There are differences, however, in the suction surface profiles.

The highest ideal critical velocity ratio for which there was no separation on the suction surface at zero jet flow was about 0.7. These curves are shown in figure 6(a). At zero jet flow there is a large peak near the leading edge. The maximum velocity occurs at about 35 percent axial chord. The velocity ratio here is 1.27, and the maximum value of the diffusion factor D_s is about 2.5. The peak is followed by a rapid diffusion to about midchord and then by a more gradual diffusion to approximately exit static pressure p_3 at the trailing edge. With a jet pressure ratio of 1.0 the pattern is similar but the peak velocity ratio and the diffusion are reduced to 1.1 and 2.0, respectively. At a jet pressure ratio of 1.5 the pressures or velocities are more nearly uniform and the entire suction surface flow is subsonic. This type of loading distribution is of the high effectiveness type because the uniform pressures on the suction surface minimize diffusion. In this case the maximum diffusion is about 1.5 but this does not all occur on the suction

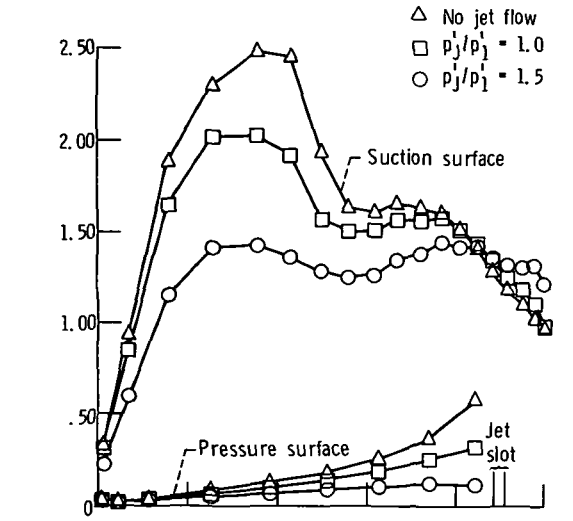

(a) Nominal ideal exit critical velocity ratio, $(V/V_{CR})_{id,3}$, 0.7.

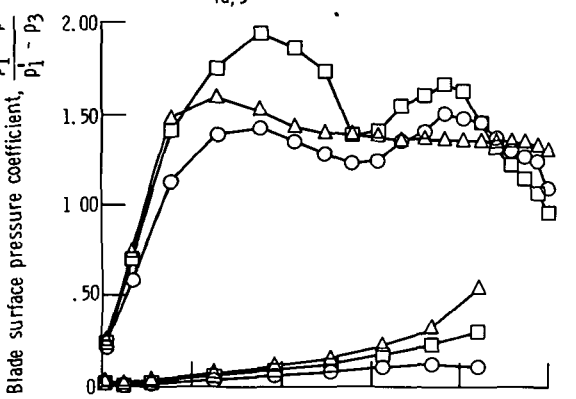

(b) Nominal exit ideal critical velocity ratio, $(V/V_{CR})_{id,3}$, 0.8.

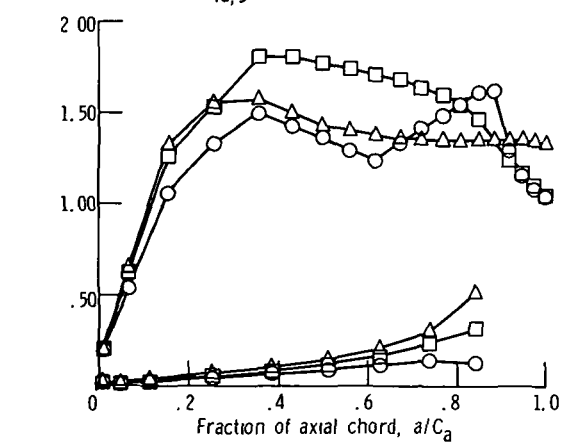

(c) Nominal exit ideal critical velocity ratio, $(V/V_{CR})_{id,3}$, 0.9.

Figure 6. - Variation of blade loading with jet flow.

surface. The suction surface pressures do not diffuse to the exit static pressure. Apparently the jet did support a difference in pressure between the pressure and suction surfaces at the trailing edge. This effect of the jet reduces the suction surface diffusion and adds an increment of loading to the after portion of the blade. The size of this added loading increment correlates with the turning of the flow due to the jet. Larger exit angles (more turning) corresponded to the larger loading increments.

The loading distributions for a nominal ideal exit critical velocity ratio of 0.8 are shown in figure 6(b). These loading distributions correspond to the blade wakes shown in figure 5. At this exit velocity ratio, and higher, the suction surface flow without the jet was separated.

The loading distribution for a jet pressure ratio of 1.5 is very similar to the one for an exit velocity ratio of 0.7. However, the suction surface pressures diffuse to a value closer to the exit static pressure. This reduces the loading increment on the aft portion of the blade. As a result, the exit angle was about 1^{o} less than it was for an exit velocity ratio of 0.7.

The loading distribution for a jet pressure ratio of 1.0 is also similar to the one shown in figure 6(a). The principal difference is a reacceleration of the flow on the suction surface following the diffusion at midchord. This reacceleration of the flow results in a larger diffusion on the aft end of the blade. This additional diffusion, however, did not have a large affect on either the loss or the exit flow angle.

Without the jet, the flow on the suction surface was separated. The separation was characterized by nearly constant static pressure over much of the suction surface and an absence of any diffusion at the trailing edge and a loss in loading compared to the unseparated case. Nevertheless, the blade loading was fairly high. The Zweifel loading coefficient was nearly as large for this condition as it was for a jet pressure ratio of 1.5. However, both flow angle and weight flow were substantially less for this condition than for attached flow. And the loss was substantially higher - about 20 percent of the ideal exit kinetic energy.

The mechanism by which the jet effects reattachment of the flow is not clear. At an exit velocity ratio of 0.8 and a jet pressure ratio of 1.0, the jet flow was about 1.4 percent of the flow entering the blade row. The tangential momentum of the jet would be a much smaller percentage of the total because of the angle of the jet slot. Surely it was too small to entrain a large separated region and pull it back onto the blade surface. The conclusion seems to be that the jet altered the flow field on both blade surfaces in such a way that it promoted reattachment.

The blade loading distributions are shown in figure 6(c) for a nominal exit ideal critical velocity ratio of 0.9. At this exit velocity it was found that the blade performance was deteriorating and the loss was increasing rapidly. The suction surface profile for zero jet flow is about the same as the corresponding profile at an exit velocity ratio of

0.8. The suction surface profiles for jet pressure ratios of 1.0 and 1.5, however, differ significantly from those at lower velocities.

At a jet pressure ratio of 1.0 there is no diffusion at midchord. Instead, the diffusion takes place gradually over most of the suction surface. The loss is more than twice as high as the loss at an exit velocity ratio of 0.8. The suction surface velocities were also very high. The maximum critical velocity ratio was 1.37 compared to 1.24 at an exit velocity ratio of 0.8. The increased loss may result from the higher velocities, but it may also result from the longer surface over which the diffusion occurred.

At a jet pressure ratio of 1.5 there was a reacceleration of the flow which was considerably more pronounced than at lower velocities. This was followed by a rapid diffusion on the aft portion of the suction surface. This diffusion extended to a pressure equal to the exit static pressure. As a result the exit angle was about 2° less than it was at an exit velocity ratio of 0.8.

Overall Performance

The overall performance of the blades is presented in terms of exit flow angle, exit flow, blade loading, and kinetic energy loss for the range of ideal exit critical velocity ratios and jet flow conditions investigated. Finally, the blade performance is compared with the design values.

Exit flow angle. - The variation of exit flow angle with exit velocity and jet flow is shown in figure 7(a). The angle data for zero jet flow is shown only for the range of exit velocity ratios for which the flow was attached to the suction surface. Up to the point of separation, the angle was nearly constant at 63°. With a jet pressure ratio of 1.0, the angle increased nearly 3°. There was a gradual decrease in the exit angle with exit velocity ratio. This amounted to 1° over the range of exit velocity ratios investigated. An increase of jet pressure ratio from 1.0 to 1.5 increased the flow angle 4° at the lowest exit velocity ratio. The flow angle, however, decreased with increasing exit velocity ratio. At an exit ideal critical velocity ratio of 0.9 the flow angle was only 1.5° larger at a jet pressure ratio of 1.5 than it was at a jet pressure ratio of 1.0. This decrease in flow angle was also reflected in the decreased loading on the aft end of the suction surface. This was discussed in the Blade Loading section.

Weight flow. - The variation of total weight flow with exit velocity and jet flow is shown in figure 7(b). In this figure, the weight flow is shown as a percentage of the design equivalent flow in order to illustrate the effect of the jet as a variable geometry device.

Weight flow data for the zero jet flow case are shown only for the range of velocity ratios where the flow was attached. For a jet pressure ratio of 1.0 the weight flow curve

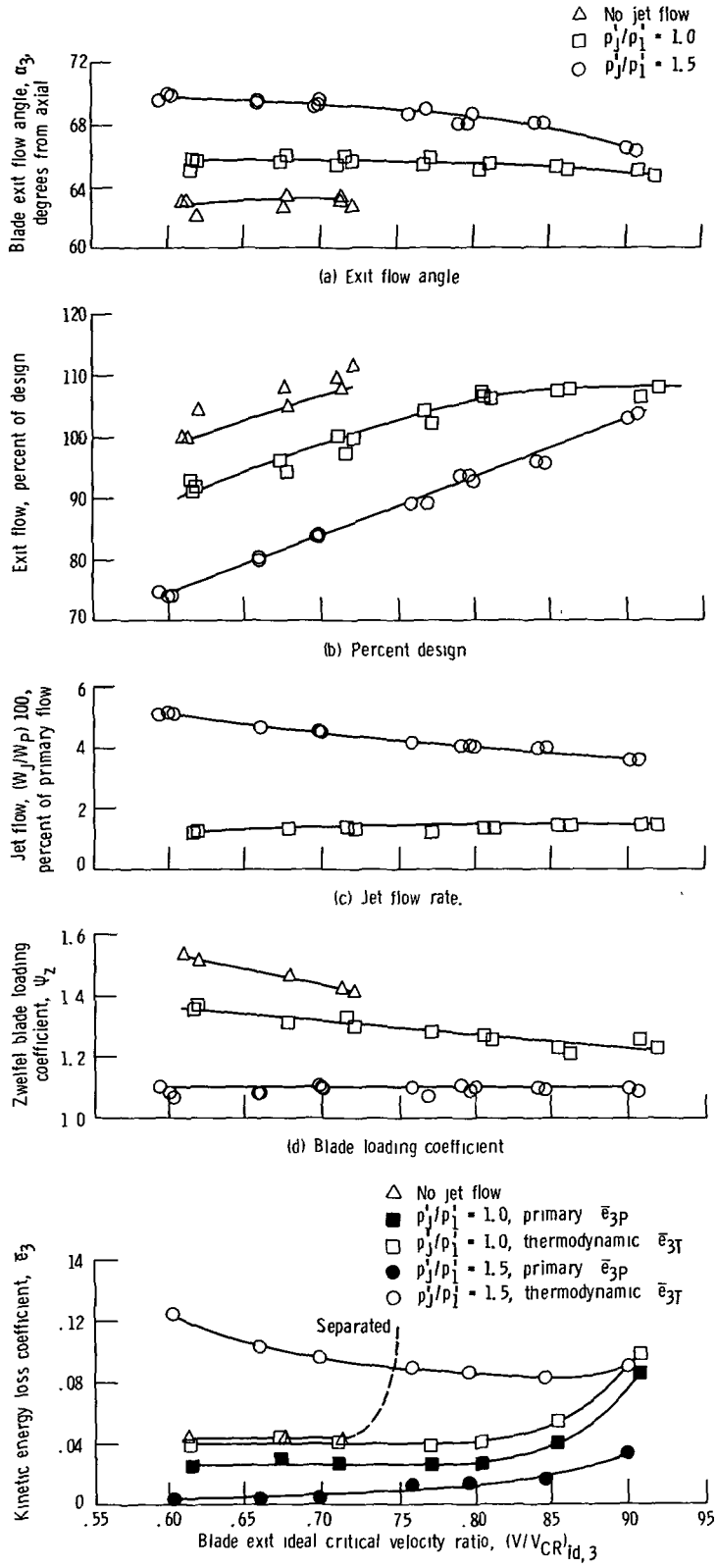

Figure 7. - Overall performance

is nearly linear up to an exit velocity ratio of 0.8. The curve then levels off abruptly indicating that the blades were choking. The linear weight flow characteristic for a jet pressure ratio of 1.5 resulted from the decrease in exit angle at higher velocities which is shown in figure 7(a).

The jet has a large influence on the weight flow. At an exit velocity ratio of 0.7 the weight flow decreased an amount equal to 8 percent of the design value between zero jet flow and a jet pressure ratio of 1.0. The flow decreased an additional 14.5 percent when the jet pressure ratio was increased to 1.5. Jet pressure ratios greater than 1.5 were found to have a proportionately smaller effect. The decrement in flow was smaller at higher velocity ratios. The flow decrement was 12.5 percent of design between jet pressure ratios of 1.0 and 1.5 at an exit velocity ratio of 0.8 but decreased rapidly to 5 percent at an exit velocity ratio of 0.9.

The variation in jet flow is shown in figure 7(c). At a jet pressure ratio of 1.0 the jet flow rate was nearly constant at about 1.4 percent of inlet flow over the range of exit velocity ratios investigated. For a jet pressure ratio of 1.5 the jet flow rate ranged from 5.1 percent of inlet flow at an exit velocity ratio of 0.6 to 3 percent at an exit velocity ratio of 0.9.

Blade loading. - The change in the Zweifel blade loading coefficient with exit velocity and jet flow is shown in figure 7(d). The Zweifel coefficients were computed by integrating the blade surface loading profiles such as those shown in figure 6.

With zero jet flow the loading coefficients were very high. They ranged from over 1.5 at the lowest exit velocity ratio to 1.4 at the highest exit velocity ratio before separation occurred. These very high loading coefficients were obtained at the cost of high suction surface velocities and diffusion with subsequent separation at comparatively low exit velocities.

A jet pressure ratio of 1.0 did reattach the flow. This jet pressure ratio also maintained attached flow to fairly high exit velocities before the blade performance began to deteriorate. The effect of the jet was to increase the exit angle and consequently decrease both weight flow and blade loading. The blade loading coefficients at a jet pressure ratio of 1.0, however, were still quite high. The downward trend of the loading coefficient occurred because the actual blade force did not increase as rapidly with exit velocity as did the ideal force.

An increase in jet pressure ratio to 1.5 resulted in a further decrease in the loading coefficient to a value of 1.1, which is still fairly high. The loading coefficient was constant at this jet pressure ratio; a consequence of the angle and weight flow characteristics.

Kinetic energy loss. - The variation of kinetic energy loss coefficient $\bar{e}_3$ with exit velocity and jet flow is shown in figure 7(e). The data shown in this figure were calculated from the results of surveys made with the short rake, 2.74 centimeters axially

downstream of the blade trailing edge. For this figure the loss coefficient is defined as one minus the ratio of the actual kinetic energy to an ideal kinetic energy at station 3. The energy of the jet flow is included in the exit ideal kinetic energy for the calculation of the thermodynamic loss $\bar{e}_{3T}$. Only the ideal energy of the primary flow is used for the calculation of the primary loss $\bar{e}_{3P}$. As a consequence, $\bar{e}_{3T}$ is larger than $\bar{e}_{3P}$ and the difference between the two increases with jet pressure ratio. For zero jet flow and for a jet pressure ratio of 1.0 where, in this case, the ideal energy of the jet and primary flow are identical, the value of the thermodynamic loss coefficient $\bar{e}_{3T}$ is the same as the loss coefficient for a blade with no second flow stream (e.g., a plain blade).

For zero jet flow and for a jet pressure ratio of 1.0, the thermodynamic loss was almost the same up to the point where the flow separated without the jet. In fact, the actual energy at station 3 was very nearly the same for all three jet flow conditions at low velocities. For a jet pressure ratio of 1.0, the loss began to increase rapidly at ideal exit critical velocity ratios greater than 0.8. With a jet pressure ratio of 1.5 the point of rapid loss increase was delayed to exit velocity ratios close to 0.9.

With a jet pressure ratio of 1.0 the design exit velocity ratio of 0.775 was achieved at an exit ideal critical velocity ratio of 0.792. At this point the thermodynamic loss was 4.2 percent. This is about the same loss that was obtained with the low solidity plain stator blades of reference 1. These blades also exhibited a rapid deterioration in performance at exit velocities higher than design.

The measured loss of the conventional solidity stator blades which served as models for the design of the jet flap blades was 2.5 percent at the mean section. A more serious consideration than the somewhat higher loss, however, is the rapid performance deterioration of low solidity blades at exit velocities higher than design. In the case of the jet flap blades, at least, the data shown in figure 7(e) for a jet pressure ratio of 1.5 indicate that the operating range of the blades can be extended to higher velocities by using higher jet pressure ratios. This may not be practical for a first-stage stator. However, the static pressure on the pressure surface of the blades near the jet slot were quite high (fig. 6). This means that the jet velocities must have been quite low. Even at a jet pressure ratio of 1.5 it is doubtful that the jet velocity ever became critical. This suggests that the effect of the jet could be increased by enlarging the jet slot and using more jet flow rather than through the use of higher jet pressure ratio. Thus it appears reasonable that the operating range of the jet flap blades could be extended to higher velocities with a jet pressure ratio of 1.0.

Comparison with design. - It is of interest to compare the actual performance of the blades with the design values. The design actual exit critical velocity ratio 0.775 occurred at an ideal value of 0.792 at a jet pressure ratio of 1.0 and a thermodynamic loss of 4.2 percent. At this point the exit flow angle was 65.5° compared to a design value of

67°. The weight flow was 5 percent greater than design. The Zweifel blade loading coefficient was 1.275 compared to a design value of 1.254.

SUMMARY OF RESULTS

The performance of a very low solidity jet-flap blade was investigated experimentally in a simple two-dimensional cascade of six blades. The following results were obtained:

1. With zero jet flow, the flow remained attached to the suction surface of the blades up to ideal exit critical velocity ratios $(V/V_{cr})_{id,3}$ of about 0.7. At higher exit velocity ratios the suction surface flow without the jet was separated. A jet to inlet total pressure ratio p_J'/p_1' of 1.0 effected reattachment and maintained attached flow up to the highest ideal exit critical velocity ratio investigated which was 0.9.

2. The effect of the jet in deflecting or turning the flow varied with both jet pressure ratio and exit velocity. At ideal exit critical velocity ratios between 0.6 and 0.7 the jet turned the flow nearly 3° between the zero jet flow case and a jet pressure ratio of 1.0. An increase in jet pressure ratio to 1.5 resulted in an additional 4° of turning. At an exit velocity ratio of 0.8 the turning decreased to 3° between jet pressure ratios of 1.0 and 1.5 and decreased to 1.5° at an exit velocity ratio of 0.9.

3. The jet had a large influence on the total weight flow. At an exit velocity ratio of 0.7 the weight flow decreased an amount equal to 8 percent of the design value between zero jet flow and a jet pressure ratio of 1.0. The flow decreased a further 14.5 percent when the jet pressure ratio was increased to 1.5. The decrement in flow was smaller at higher velocity ratios. The flow decrement was 12.5 percent of design between jet pressure ratios of 1.0 and 1.5 at an exit velocity ratio of 0.8 and decreased rapidly to 5 percent at an exit velocity ratio of 0.9. The jet flow rate was nearly constant at about 1.4 percent of inlet flow at a jet pressure ratio of 1.0 and ranged from 5.1 to 3.6 percent of inlet flow at a jet pressure ratio of 1.5 over the range of exit velocity ratios investigated.

4. Very high blade loading was obtained. The Zweifel blade loading coefficient ψ_z was as high as 1.5 without jet flow. With jet flow, blade loading decreased with jet pressure ratio. The Zweifel blade loading coefficient at a jet pressure ratio of 1.0 varied between 1.36 and 1.23 for the range of exit velocity ratios investigated. With a jet pressure ratio of 1.5 the blade loading coefficient was constant at 1.1.

5. The thermodynamic loss at design exit critical velocity ratio and a jet pressure ratio of 1.0 was 4.2 percent of the ideal exit kinetic energy. The loss of the conventional solidity stator blades which served as a model for the jet flap blade was 2.5 percent at the mean section. For a jet pressure ratio of 1.0 the loss of the jet flap blade began to

increase rapidly at ideal exit critical velocity ratios greater than 0.8. With a jet pressure ratio of 1.5 the point of rapid loss increase was delayed to exit velocity ratios close to 0.9.

Lewis Research Center,
National Aeronautics and Space Administration,
Cleveland, Ohio, August 31, 1971,
764-74.

REFERENCES

1. Stabe, Roy G.: Design and Two-Dimensional Cascade Test of Turbine Stator Blade with Ratio of Axial Chord to Spacing of 0.5. NASA TM X-1991, 1970.

2. Nosek, Stanley M.; and Kline, John F.: Two-Dimensional Cascade Investigation of a Turbine Tandem Blade Design. NASA TM X-1836, 1969.

3. Lueders, H. G.; and Roelke, R. J.: Some Experimental Results of Two Concepts Designed to Increase Turbine Blade Loading. Paper 69-WA/GT-1, ASME, Nov. 1969.

4. Bettner, James L.; and Nosek, Stanley M.: Summary of Tests on Two Highly Loaded Turbine Blade Concepts in Three-Dimensional Cascade Sector. Paper 69-WA/GT, ASME, Nov. 1969.

5. Nosek, Stanley M.; and Kline, John F.: Two-Dimensional Cascade Test of a Jet-Flap Turbine Rotor Blade. NASA TM X-2183, 1971.

6. Whitney, Warren J.; Szanca, Edward M.; Moffitt, Thomas P.; and Monroe, Daniel E.: Cold-Air Investigation of a Turbine for High-Temperature-Engine Application. 1. Turbine Design and Overall Stator Performance. NASA TN D-3751, 1967.

7. Zweifel, O.: The Spacing of Turbo-Machine Blading, Especially with Large Angular Deflection. Brown Boveri, Rev., vol. 32, no. 12, Dec. 1945, pp. 436-444.

8. Miser, James W.; Stewart, Warner L.; and Whitney, Warren J.: Analysis of Turbomachine Viscous Losses Affected by Changes in Blade Geometry. NACA RM E56F21, 1956.

9. Katsanis, Theodore: FORTRAN Program for Calculating Transonic Velocities on a Blade-to-Blade Stream Surface of a Turbomachine. NASA TN D-5427, 1969.

NASA-Langley, 1971 — 1 E-6479

"The aeronautical and space activities of the United States shall be conducted so as to contribute . . . to the expansion of human knowledge of phenomena in the atmosphere and space. The Administration shall provide for the widest practicable and appropriate dissemination of information concerning its activities and the results thereof."

—NATIONAL AERONAUTICS AND SPACE ACT OF 1958

NASA SCIENTIFIC AND TECHNICAL PUBLICATIONS

TECHNICAL REPORTS: Scientific and technical information considered important, complete, and a lasting contribution to existing knowledge.

TECHNICAL NOTES: Information less broad in scope but nevertheless of importance as a contribution to existing knowledge.

TECHNICAL MEMORANDUMS: Information receiving limited distribution because of preliminary data, security classification, or other reasons.

CONTRACTOR REPORTS: Scientific and technical information generated under a NASA contract or grant and considered an important contribution to existing knowledge.

TECHNICAL TRANSLATIONS: Information published in a foreign language considered to merit NASA distribution in English.

SPECIAL PUBLICATIONS: Information derived from or of value to NASA activities. Publications include conference proceedings, monographs, data compilations, handbooks, sourcebooks, and special bibliographies.

TECHNOLOGY UTILIZATION PUBLICATIONS: Information on technology used by NASA that may be of particular interest in commercial and other non-aerospace applications. Publications include Tech Briefs, Technology Utilization Reports and Technology Surveys.

Details on the availability of these publications may be obtained from:

SCIENTIFIC AND TECHNICAL INFORMATION OFFICE

NATIONAL AERONAUTICS AND SPACE ADMINISTRATION

Washington, D.C. 20546